



INTEGRATED
LABORATORY

Volume 1, 2022

PROCEEDING

of International Conference
of Education, Sciences, Technology, Engineering, & Mathematics

"Naturan Sciences, Mathematics, Technology, and Education for Humanity and Civilization"

Semarang, June 28th-29th, 2022



The author is solely responsible for the articles published in this proceeding, either in part or whole.

PROCEEDING OF INTERNATIONAL CONFERENCE OF EDUCATION, SCIENCES, TECHNOLOGY, ENGINEERING, & MATHEMATICS

"NATURAL SCIENCES, MATHEMATICS, TECHNOLOGY, AND EDUCATION
FOR HUMANITY AND CIVILIZATION"

xi, 313 page

ISSN: 2985-5721

Fakultas Sains dan Teknologi
Universitas Islam Negeri Walisongo Semarang
Indonesia
September 2022

A. Steering Committee

Dr. H. Ismail, M.Ag.
Dr. H. Saminanto, M.Sc.
Dr. H. Nur Khoiri, M.Ag.
Dr. Hj. Nur Khasanah, M.Kes.
Muh. Kharis, S.H., M.H.

B. Organizing Comitee

Head of Comitee	: Teguh Wibowo, M.Pd.
Secretary	: Rina Susi Cahyawati, M.Pd. Arifah Purnamaningrum, M.Sc.
Treasurer	: Julia Mardhiya, M.Pd. Ndzani Latifatur Rofi'ah, M.Pd.
Event Division	: Prihadi Kurniawan, M.Sc. Istikomah, M.Sc. Wiwik Kartika Sari, M.Pd.
Publication	: Andang Prasetyo, S.Pd. Ghani Ghaffar Garaudy, S.Pd. Ahmad Minanur Rohim, M.Pd. Ahmad Mughis, S.Pd.
Public Relations	: Ariska Kurnia Rachmawati, M.Sc. Mutista Hafshah, M.Si.



LIST OF CONTENT

Preface	iii
List of Content	v
Problems of Online Learning and the Use of Smartphones in Physics Learning at Cirebon, West Java Rida Sholihah, Parlindungan Sinaga, Wawan Setiawan	(1-5)
Development of Scientific Literacy-Based Test Instruments Characterized by Local Wisdom Using the Quizizz Application for Optical Materials Ida Puji Astuti, Joko Budi Poernomo, Qisthi Fariyani	(6-9)
Effectiveness of Augmented Reality in Physics Laboratory Experiments: a Literature Review Darta Harpian, Irma Rahma Suwarma, Achmad Samsudin	(10-14)
The effectiveness of The Treffinger Learning Model on Student's Metacognitive Ability on Work and Energy Materials of Grade X SMA I Simanjaya Siti Nur Rofikoh, Susilawati, Edi Daenuri Anwar	(15-18)
The Urgency of Science – Religious Learning: Literature Review Edi Daenuri Anwar, Wiyanto, Ani Rusilowati, Endang Susilaningsih	(19-24)
Classification of Normal, Benign, and Malignant Breast on Mammographic Images Based on Texture Characteristics Using Multi-Layer Perceptron (MLP) Method Alvania Nabila Tasyakuranti, Fahira Septiani, Heni Sumarti	(25-31)
Development of Telemedicine System to Measure Blood Sugar, Cholesterol, and Uric Acid Levels with Non Invasive Method as A Prevention Fahira Septiani, Alvania Nabila Tasyakuranti, Heni Sumarti	(32-36)
Neutrino Mass Generation in a Minimal Extension of The Standars Model Using The Type-I Seesaw Mechanism Siti Romzatul Haniah, Istikomah, Muhammad Ardhi Khalif, Hamdan Hadi Kusuma	(37-39)
IoT-Based Water Cooling Practice Design Agus Sudarmanto, Fachrizal Rian Pratama, Khoerul Mutaqin	(40-45)



- Singularity Study on Weyl-Lewis-Papapetrou (WLP) Metrics with Schwarzschild Metric Background (46-48)
Try Adi Sucipto, M. Ardhi Khalif, Irman Said Prastyo, Istikomah
- Development Electronic Module Oriented Multiple Chemical Representation in Chemical Bond Lesson (49-53)
Bayu Pranata, Atik Rahmawati, Resi Pratiwi
- The Effect of Using Augmented Reality-Based Learning Media on Students's Concept Understanding on Molecular Shape (54-57)
Febrian Solikhin, Dewi Handayani, Salastri Rohiat
- Learning Style Relationship and Study Results on Quizizz-Assisted Stoichiometry Material (58-61)
Sania Rahmatika, Apriliana Drastisianti, Sri Mulyanti
- Electronic Module Colligative Properties of Solutions Integrated Green Chemistry for Real Life: Literature Review (62-67)
Melisa Nur Kibtiah, Sri Mulyanti
- Response to Redox Learning Videos (Tips and Tricks for Easy Problem Solving) (68-72)
Adistya Maranatha Ummah, Sri Mulyanti
- The Effectiveness of the STAD Type Cooperative Learning Model Assisted by Bridge Cards to Improve Student Learning Outcomes (73-77)
Thoha Mukhtar, Resi Pratiwi, Teguh Wibowo
- Development of Video Media for Learning Electrolyte & Non-Electrolyte Solutions Based on Green Chemistry (78-84)
Ismi Yaomil Auliya, Teguh Wibowo, Lenni Khotimah Harahap
- Constraints In The Mirror Model Modified During The Big Bang Nucleosynthesis Era (85-89)
Istikomah, Nurul Embun Isnawati, Heni Sumarti, Irman Said Prastyo
- Free Radical Review: Cadmium as Inorganic Pollution, Volatile Organic Compounds, and Cosmetic Preservatives as Causing Agent of Increased ROS (93-98)
Aden Dhana Rizkita, Sintia Ayu Dewi, Nurlita Julianti, Anna Uswatun Hasanah Rochjana
- Preliminary Treatment Comparative Evaluation Against Physicochemical Properties Edamame Flour (*Glicine max (L) Merrill*) (99-102)
Subandi, Chandra Utami Wirawati, Dwi Eva Nirmagustina

Constraints In The Mirror Model Modified During The Big Bang Nucleosynthesis Era

Istikomah^{1*}, Nurul Embun Isnawati², Heni Sumarti³, Irman Said Prastyo⁴

^{1,2,3,4} Department of Physics, UIN Walisongo Semarang

*Corresponding author. Email: istikomah@walisongo.ac.id

ABSTRACT

The Big Bang Nucleosynthesis (BBN) was the stage in the universe's evolution when helium-4 was produced. According to BBN theory, there are Constraints to all standard model extensions. Assuming in the Modified Mirror Model, the temperature of the real sector is the same as the mirror sector after warming back after inflation, $T_i = T'_i = 10^{13} \text{ GeV}$. When the Big Bang Nucleosynthesis occurs, several massive particle decay processes can cause a temperature difference between the real and mirror sectors. The temperature ratio between mirror sectors is $\cong 0.03 - 0.05$ with the lower bound of the mass ratio of real and mirror scalar fields $m_{\phi_e}/m_{\phi_{eE}} \cong 0.5$.

Keywords: Standard Model, Big Bang Nucleosynthesis, Mirror Model, Particle Physics, Feynman Diagram

1. INTRODUCTION

One of the stages of the universe's evolution is the production of past light nuclei known as Big Bang Nucleosynthesis (BBN) era. The ongoing process of BBN is explained by the Standard BBN theory, which consists of the Particle Physics Standard Model and the Cosmological Standard Model. BBN theory predicts that at about one MEV, a quarter of the universe was dominated by relic abundances of helium-4 [1]. The prediction of the BBN theory provides constraints on the number of light particles at BBN temperatures. If there are light particles whose masses are in the same order as neutrinos in the mass of BBN, the number of additions allowed is only one [2]. The BBN theory follows the results of extrapolating observational data; the other relativistic particles allowed are around $\Delta N < 0.2 - 0.3$ [3]. This additional light particle is only possible if the particle temperature is lower than the photon temperature.

The Standard Particle Model can predict the masses of the W^\pm and Z^0 bosons. However, it cannot explain dark matter, particle-antiparticle asymmetry, and mass hierarchy. Several expansions of the Standard Model, such as the $SU(5)$ grand unified theory with A 4 modular symmetry [4], Minimal Left-Right Supersymmetry Model [5], Minimal Extension of the Standard Model [6], Modified Left-Right Symmetry Model [7][8][9] and other models. that hope can solve the problem. Massive particle decay with a lifetime of 10^{-2} s has been examined, and did not affect the abundance of relic Helium-4 [10]. A model with massive neutral lepton

decay has been examined; this Model managed to avoid the problem of BBN with a particle lifetime of less than $0,02 \text{ s}$ [11]. In the modified mirror model, there is a mirror sector; there are mirror particles that have the potential to affect the abundance of past light nuclei. Thus, it is necessary to analyze the BBN constraints on the modified mirror model.

2. THE MODEL

The Modified Mirror Model is built based on the gauge group $SU(3)_1 \otimes SU(3)_2 \otimes SU(2)_L \otimes SU(2)_R \otimes U(1)_Y \otimes U(1)_X$. The list of particles in this model is shown in Table 1

Table 1. Particle with the Fundamental Representative

Real Sector	Representative	Mirror Sector	Representative
ℓ_L	1,1,2,1,-1,-1	L_R	1,1,2,1,-1,1
ν_R	1,1,1,1,0,0	N_L	1,1,1,1,0,0
e_R	1,1,1,1,-2,-2	E_L	1,1,1,1,-2,-2
q_L	$3,1,2,1,\frac{1}{3},\frac{1}{3}$	Q_R	$3,1,2,1,\frac{1}{3},-\frac{1}{3}$
u_R	$3,1,1,1,\frac{4}{3},\frac{4}{3}$	U_R	$3,1,1,1,\frac{4}{3},-\frac{4}{3}$
d_R	$3,1,1,1,-\frac{2}{3},-\frac{2}{3}$	D_R	$3,1,1,1,-\frac{2}{3},2$
χ_L	1,1,2,1,-1,-1	χ_R	1,1,2,1,-1,1
ϕ_e	1,1,1,1,-2,-2	ϕ_E	1,1,1,1,-2,-2

The scalar field potential that describes the interaction between the most common scalar fields that is invariant to the gauge transformation is shown by Equation (1)

$$V_H = -\mu_1^2(|\chi_L|^2 + |\chi_R|^2) - \mu_2^2(|\phi_e|^2 + |\phi_E|^2) + \lambda_1(|\chi_L|^4 + |\chi_R|^4) + \lambda_2(|\phi_e|^4 + |\phi_E|^4) + \alpha_1|\chi_L|^2|\chi_R|^2 + \alpha_2|\phi_e|^2|\phi_E|^2 + \alpha_3(|\chi_L|^2|\phi_e|^2 + |\chi_R|^2|\phi_E|^2) + \alpha_4(|\chi_L|^2|\phi_e|^2 + |\chi_R|^2|\phi_E|^2) \quad (1)$$

Yukawa's interaction most common restriction on these modified mirror models is shown by Equation (2)

$$L \supset G_e(\bar{\ell}_L \chi_L^c e_R + \bar{L}_R \chi_R^c) - G_\nu(\bar{\ell}_L \chi_L \nu_R + \bar{L}_R \chi_R N_L) - G_d(\bar{q}_L \chi_L^c d_R + \bar{Q}_R \chi_R^c D_L) - G_u(\bar{q}_L \chi_L u_R + \bar{Q}_R \chi_R U_L) - G_{\nu e}(\bar{e}_R \phi_e N_L + \bar{E}_R \phi_E \nu_R) - G'_{\nu e}(\bar{e}_R \phi_e \nu_R^c + \bar{E}_R \phi_E N_L^c) - G'_\nu(\bar{\ell}_L \chi_L N_L^c - \bar{L}_R \chi_R \nu_R^c) - M_m(\bar{\nu}_R^c \nu_R - \bar{N}_L^c N_L) - M_d \bar{N}_L \nu_R + h.c. \quad (2)$$

Equation (2) describes this Model's interaction between fermions and the scalar field.

3. TEMPERATURE EVOLUTION

Based on the modified mirror model, BBN occurs when the universe is dominated by radiation energy density. The expansion rate of the universe is shown by Equation (3)

$$H^2 = \frac{8\pi}{3m_{pl}^2}(\rho_n + \rho_c) \quad (3)$$

Where ρ_n is the energy density of the real sector, and ρ_c is the energy density of the mirror sector. The different energy densities of the particles in the mirror sector will certainly affect the production of relic helium-4. According to BBN theory, the additional relativistic degrees of freedom that can still be tolerated are $\Delta g_* = 1.75$ with $\Delta N = 1$. For this Model to satisfy the BBN constraint, the temperature of the mirror sector must be lower. Thus Equation (3) turns into Equation (4)

$$H^2 = \frac{8\pi}{3m_{pl}^2} g_* \frac{\pi^2}{30} T^4 \left(1 + \frac{g'_* T'^4}{g_* T^4}\right) \quad (4)$$

It is assumed that the particles of the real sector and the mirror sector do not interact with each other. The interaction that may occur is the decay process of the massive particles in each sector released from thermal equilibrium. The decay process contributes entropy, the amount of which can be determined using the laws of thermodynamics as shown by the Equation (5)

$$S^{\frac{1}{3}} \dot{S} = \sum_k \frac{\left(\frac{2\pi^2}{45} g_*\right)^{\frac{1}{3}} R^4 \rho_k}{\tau_k} \quad (5)$$

By solving equation (5) it can be obtained the entropy ratio of the final condition ($t \gg \tau$) to the initial condition ($t \ll \tau$) per comoving volume shown by Equation (6)

$$\left(\frac{S_f}{S_i}\right)^{\frac{4}{3}} \cong 2.42 \sum_k \frac{(m_k Y_{ki})^{\frac{4}{3}} g_*^{\frac{1}{3}} \tau_k^{\frac{2}{3}}}{m_{pl}^{\frac{2}{3}}} \quad (6)$$

In the period after post-inflation reheating, the temperature of the real and mirror sectors is the same, namely $10^{13} GeV$. At this temperature, the energy density of the two sectors is dominated by non-relativistic massive particles, namely ν_R and N_L . The effective masses of the two particles are almost the same as the temperature at that time. Flavor base particle ν_R and N_L can be written in mass basis, $\nu_R = P_R \nu'$ and $N_L = P_L N'$. Based on the Yukawa interaction term, the possible decay processes of the particles ν' and N' are shown in Table 2.

Table 2. Neutrino Decay Modes

ν' decay modes	N' decay modes
(a) $\nu' \rightarrow \ell + \chi_L$	(e) $N' \rightarrow \ell + \chi_L$
(b) $\nu' \rightarrow L + \chi_R$	(f) $N' \rightarrow L + \chi_R$
(c) $\nu' \rightarrow E' + \phi_E$	(g) $N' \rightarrow E + \phi_E$
(d) $\nu' \rightarrow e + \phi_e$	(h) $N' \rightarrow e + \phi_e$

The neutrino decay modes in table 2 are illustrated via the Feynman diagram, as shown in Figure 1. Then the decay interaction rate is analyzed using the Golden Rule[12].

The temperature ratio after and before the particles ν' and N' decays into real relativistic particles with effective relativistic degrees of freedom in the real sector $g_{*I} = 108.75$ shown by the Equation (7)

$$\left(\frac{T_{fI}}{T_{iI}}\right)^4 \cong 0.018 \frac{m_{\nu'}^{\frac{2}{3}}}{g_{*I} m_{pl}^{\frac{2}{3}}} (G_\nu^2 + G_{\nu e}^2)^{-\frac{2}{3}} \quad (7)$$

While the temperature ratio in the mirror sector with relativistic degrees of freedom $g'_{*I} = 108.75$ is shown by the Equation (8)

$$\left(\frac{T'_{fI}}{T'_{iI}}\right)^4 \cong 0.018 \frac{m_{N'}^{\frac{2}{3}}}{g'_{*I} m_{pl}^{\frac{2}{3}}} (G_\nu^2 + G_{\nu e}^2)^{-\frac{2}{3}} \quad (8)$$

The final temperature ratio of the two sectors shown in Equations (7) and (8) is only distinguished by the mass ν' and N' . However, because at the beginning, it was assumed that the effective period was the same, the final temperature in the first stage, the temperature in both sectors is the same, $T_{fI} = T'_{fI}$.

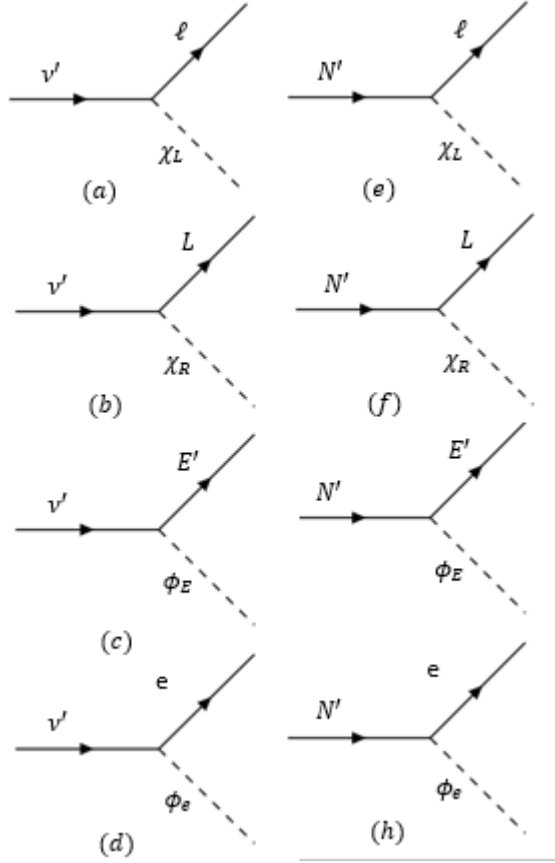


Figure 1. Feynman Diagram of Neutrino Decay Modes

After the universe's temperature decreased by about 10^4 GeV, the scalar fields ϕ_e and ϕ_E acquired unequal vacuum expectation values (VEV). The scalar field ϕ_e takes a VEV of $\langle \phi_e \rangle = 0$, while $\langle \phi_E \rangle = \frac{1}{2} v_{\phi_E}$ so the mass of the scalar field is not the same $m_{\phi_e} \neq m_{\phi_E}$. At this stage, the prospective mirror photon gains mass. The possible decay processes of the particles ϕ_e, ϕ_E and γ_D are shown in the table 3 and 4.

Table 3. ν' and N' Mediated Decays

ν' Mediated Decay	N' Mediated Decay
(a') $h_{\phi_e} \rightarrow e + \bar{l} + \chi_L^*$	(e') $h_{\phi_e} \rightarrow e + \bar{l} + \chi_L^*$
(b') $h_{\phi_E} \rightarrow E' + \bar{l} + \chi_L^*$	(f') $h_{\phi_E} \rightarrow E' + \bar{l} + \chi_L^*$
(c') $h_{\phi_e} \rightarrow e + \bar{L} + \chi_R^*$	(g') $h_{\phi_e} \rightarrow e + \bar{L} + \chi_R^*$
(d') $h_{\phi_E} \rightarrow E' + \bar{L} + \chi_R^*$	(h') $h_{\phi_E} \rightarrow E' + \bar{L} + \chi_R^*$

Table 4. Direct Decays

Direct Decay
(i') $h_{\phi_E} \rightarrow \chi_R + \chi_R$
(j') $h_{\phi_E} \rightarrow \chi_L + \chi_L$
(k') $\gamma_D \rightarrow \bar{f}' + f'$

The (a'), (b'), (e') and (f') decay modes are the decay of the scalar fields ϕ_e and ϕ_E mediated by

neutrinos ν' whose decay results contribute entropy in the real sector. At the same time, the results of the mode decay (c'), (d'), (g') and (h') contribute entropy in the mirror sector. The Feynman diagram illustrating the direct decay mode can be seen in Figure 2.

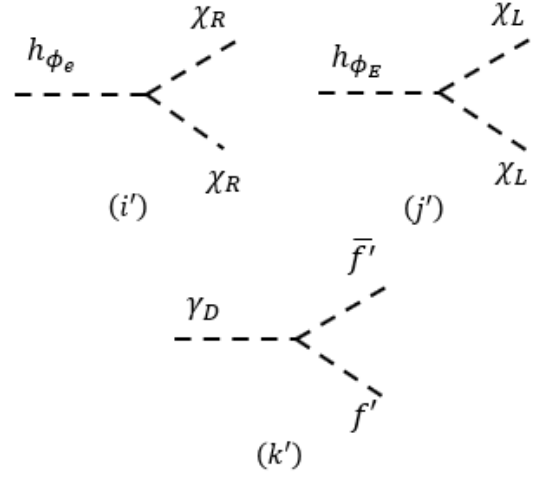


Figure 2 Feynman Diagram of Direct Decays

The temperature ratio in the real sector after ($t \gg \tau_{\phi_e}$) and before ($t \ll \tau_{\phi_e}$) the scalar fields ϕ_e and ϕ_E decays into relativistic particles with relativistic degrees of freedom at this stage $g_{*II} = 106.75$ is shown by Equation (9)

$$\left(\frac{T'_{fII}}{T'_{iII}}\right)^4 \cong 61.42 \frac{(G_{ve}^2 G_v^2)^{-\frac{2}{3}} m_{\nu'}^{\frac{4}{3}}}{g_{*I} m_{pl}^{\frac{2}{3}} m_{\phi_e}^4} \left[m_{\phi_e}^{\frac{10}{3}} + m_{\phi_E}^{\frac{10}{3}} \left(\frac{9(8\pi)^3 \alpha_3^2 m_{\nu'}^2}{4\pi \lambda_2 G_{ve}^2 G_v^2 m_{\phi_E}^2} \right)^{-\frac{2}{3}} \right] \quad (9)$$

Meanwhile, the temperature ratio after ($t \gg \tau_{\phi_E}$) and before ($t \ll \tau_{\phi_E}$) the field ϕ_e, ϕ_E , and the mirror photon γ_D decays in the mirror sector with $g'_{*II} = 104.75$ shown by Equation (10)

$$\left(\frac{T'_{fII}}{T'_{iII}}\right)^4 \cong 61.42 \frac{(G_{ve}^2 G_v^2)^{-\frac{2}{3}} m_{\nu'}^{\frac{4}{3}}}{g_{*I} m_{pl}^{\frac{2}{3}} m_{\phi_e}^4} \left[\frac{m_{\phi_e}^{\frac{10}{3}}}{2^{2/3}} + m_{\phi_E}^{\frac{10}{3}} \left(\frac{9(8\pi)^3 \alpha_3^2 m_{\nu'}^2}{4\pi \lambda_2 G_{ve}^2 G_v^2 m_{\phi_E}^2} \right)^{-\frac{2}{3}} \right] + M_{\gamma_D}^{\frac{16}{3}} \left((8\pi)^3 \sum_f \frac{Q_{Df}^2 m_{N'}^2 M_{\gamma_D}}{48\pi G_{ve}^2 G_v^2} \right)^{-\frac{2}{3}} \quad (10)$$

The ratio of the final temperature of the first stage to the final temperature of the second stage is shown by the Equation (11)

$$\left(\frac{T'_{fII}}{T'_{fIII}}\right)^4 \cong \frac{g_{*I} g_{*II} m_{\phi_e}^4}{g'_{*I} g'_{*II} m_{\phi_E}^4} \left\{ \frac{\frac{10}{3} m_{\phi_e}^{\frac{10}{3}} + m_{\phi_E}^{\frac{10}{3}} \left(\frac{9(8\pi)^3 \alpha_3^2 m_{\nu'}^2}{4\pi \lambda_2 G_{\nu_e}^{\prime 2} G_{\nu'}^{\prime 2} m_{\phi_E}^2} \right)^{-\frac{2}{3}}}{m_{\phi_e}^{\frac{10}{3}} + m_{\phi_E}^{\frac{10}{3}} \left(\frac{9(8\pi)^3 \alpha_3^2 m_{\nu'}^2}{4\pi \lambda_2 G_{\nu_e}^{\prime 2} G_{\nu'}^{\prime 2} m_{\phi_E}^2} \right)^{-\frac{2}{3}}} + \frac{M_{\gamma_D}^{\frac{16}{3}} \left((8\pi)^3 \sum_f \frac{Q_{Df}^2 m_{N'}^2 M_{\gamma_D}}{48\pi G_{\nu_e}^{\prime 2} G_{\nu'}^{\prime 2}} \right)^{-\frac{2}{3}}}{m_{\phi_e}^{\frac{10}{3}} + m_{\phi_E}^{\frac{10}{3}} \left(\frac{9(8\pi)^3 \alpha_3^2 m_{\nu'}^2}{4\pi \lambda_2 G_{\nu_e}^{\prime 2} G_{\nu'}^{\prime 2} m_{\phi_E}^2} \right)^{-\frac{2}{3}}} \right\} \quad (11)$$

The difference in the temperature of the two sectors is in the next stage. The degrees of freedom in the real sector, real photons are still massless and relativistic, while mirror photons are mass and become non-relativistic.

When the temperature of the universe decreased by about 10^2 GeV, the scalar fields χ_L and χ_R acquired the same VEV, $\langle \chi_L \rangle = \langle \chi_R \rangle = v$. This causes the scalar field mass χ_L to equal χ_R , $m_{\chi_L} = m_{\chi_R}$. Thus, all scalar fields have acquired their VEV and mass at this stage. At this time, degrees of freedom are decreasing because the scalar fields χ_L and χ_R are no longer relativistic. The magnitude of the degree of relativity in the real sector at this stage is $g_{*III} = 105.75$. change in the temperature of the real sector, indicated by the Equation (12)

$$\left(\frac{T'_{fIII}}{T_{III}}\right)^4 \cong 1.67 \frac{m_{\chi_L}^{\frac{2}{3}}}{g_{*III} m_{pl}^{\frac{2}{3}}} (G_e^2 + G_d^2 + G_u^2)^{-\frac{2}{3}} \quad (12)$$

In the mirror sector, the temperature ratio after the scalar field χ_R decays, $t \gg \tau_{\chi_L}$ compared to before the scalar field χ_R decays into mirror particles with relativistic degrees of freedom in this sector $g_{*III} = 103.75$ is shown by Equation (13)

$$\left(\frac{T'_{fIII}}{T'_{III}}\right)^4 \cong 1.67 \frac{m_{\chi_R}^{\frac{2}{3}}}{g_{*III} m_{pl}^{\frac{2}{3}}} (G_e^2 + G_d^2 + G_u^2)^{-\frac{2}{3}} \quad (13)$$

The final temperature ratio in the final stage until BBN takes place between the two sectors with the assumption $T_{II} = T'_{II}$ is shown by the Equation (14)

$$\left(\frac{T'_{fIII}}{T'_{fIII}}\right)^4 \cong \frac{g_{*I} g_{*II} g_{*III} m_{\phi_e}^4}{g'_{*I} g'_{*II} g'_{*III} m_{\phi_E}^4} \left\{ \frac{\frac{10}{3} m_{\phi_e}^{\frac{10}{3}} + m_{\phi_E}^{\frac{10}{3}} \left(\frac{9(8\pi)^3 \alpha_3^2 m_{\nu'}^2}{4\pi \lambda_2 G_{\nu_e}^{\prime 2} G_{\nu'}^{\prime 2} m_{\phi_E}^2} \right)^{-\frac{2}{3}}}{m_{\phi_e}^{\frac{10}{3}} + m_{\phi_E}^{\frac{10}{3}} \left(\frac{9(8\pi)^3 \alpha_3^2 m_{\nu'}^2}{4\pi \lambda_2 G_{\nu_e}^{\prime 2} G_{\nu'}^{\prime 2} m_{\phi_E}^2} \right)^{-\frac{2}{3}}} + \frac{M_{\gamma_D}^{\frac{16}{3}} \left((8\pi)^3 \sum_f \frac{Q_{Df}^2 m_{N'}^2 M_{\gamma_D}}{48\pi G_{\nu_e}^{\prime 2} G_{\nu'}^{\prime 2}} \right)^{-\frac{2}{3}}}{m_{\phi_e}^{\frac{10}{3}} + m_{\phi_E}^{\frac{10}{3}} \left(\frac{9(8\pi)^3 \alpha_3^2 m_{\nu'}^2}{4\pi \lambda_2 G_{\nu_e}^{\prime 2} G_{\nu'}^{\prime 2} m_{\phi_E}^2} \right)^{-\frac{2}{3}}} \right\} \quad (14)$$

The temperature difference between sectors is maintained until the ancient helium formation occurs. The real sector temperature is higher than the mirror sector temperature[13].

4. BBN CONSTRAINTS

The temperature ratio between sectors in Equation (14) persists until the universe's temperature reaches 1 MeV. The second term of the Equation (14) is so small compared to the first term that it can be neglected. Through this approach, the temperature ratio between the two sectors while the BBN process takes place is shown by the Equation (15)

$$\left(\frac{T'_{fIII}}{T_{fIII}}\right)^4 \cong \frac{g_{*I} g_{*II} g_{*III} m_{\phi_e}^4}{g'_{*I} g'_{*II} g'_{*III} m_{\phi_E}^4} \frac{\left[2^{-\frac{2}{3}} m_{\phi_e}^{\frac{10}{3}}\right]}{\left[m_{\phi_E}^{\frac{10}{3}}\right]} \quad (15)$$

In the modified mirror model, the mirror particle still relativistic when BBN takes place is mirror neutrino N_R and mirror electron E_L because the masses of the two mirror particles are in the same order as the real light neutrino mass ν_L . So, the additional effective relativistic degrees of freedom when BBN takes place is shown by Equation (16)

$$\Delta g_* = \frac{7}{8} [3_N(2) + 3_E(2)] \left(\frac{T'}{T}\right)^4 \quad (16)$$

Other particles still relativistic when BBN occurs are three mirror sector neutrinos and three electron leptons, muons, and mirror sector tausons. The temperature ratio between the mirror sector and the real sector, according to the BBN constraint, is shown by Equation (17)

$$\left(\frac{T'_f}{T_f}\right)^4 \cong 0.03 - 0.05 \quad (17)$$

By substituting the lower limit of the temperature ratio (17) into Equation (15), it gave the mass ratio of the scalar field ϕ_e and ϕ_E is obtained, as shown by Equation (18)

$$\frac{m_{\phi_e}}{m_{\phi_E}} \cong 0.5 \quad (18)$$

The ratio of the scalar field masses ϕ_e and ϕ_E in Equation (18) guarantees that the additional particle-particles introduced in the modified mirror model do not affect the abundance of primordial helium-4. So, this model satisfies the BBN constraints.

5. CONCLUSION

In the modified mirror model, particle decay occurs after post-inflation reheating until the BBN mass continues, which causes the temperature in the mirror sector to be lower than in the real sector. This model satisfies the BBN constraints with the condition that the lower limit of the mass ratio of the scalar fields ϕ_e and ϕ_E is about 0.5.

REFERENCES

- [1] V. A. Rubakov and S. Gorbunov, D., *Introduction to The Theory Of The Early Universe Hot Big Bang Theory*. World Scientific, 2011.
- [2] E. W. Kolb and M. S. Turner, *The Early Universe*. New york: Addison-Wesley Publishing Company, 1990.
- [3] V. Berezhinsky, M. Narayan, and F. Vissani, "Mirror model for sterile neutrinos," *Nucl. Phys. B*, vol. 658, no. 1–2, pp. 254–280, 2003, doi: 10.1016/S0550-3213(03)00191-3.
- [4] F. J. de Anda, S. F. King, and E. Perdomo, "S U (5) grand unified theory with A 4 modular symmetry," *Phys. Rev. D*, vol. 101, no. 1, p. 15028, 2020, doi: 10.1103/physrevd.101.015028.
- [5] K. Huitu, "A minimal supersymmetric left-right model, dark matter and signals at the LHC," *Eur. Phys. J. Spec. Top.*, 2020.
- [6] S. R. Haniah, Istikomah, M. A. Khalif, and H. H. Kusuma, "Scalar Field Mass Generation in the Gauge Theory SU(2)XU(1)XZ2," *J. Phys. Conf. Ser.*, 2020.
- [7] Istikomah, "Pembangkitan Massa Medan Skalar dan Boson Tera pada Model Simetri Kiri Kanan Termodifikasi Berdasarkan Grup Tera SU(3)⊗SU(2)_L⊗SU(2)_R⊗U(1)_Y," *J. Fis.*, vol. 10, no. 2, pp. 35–41, 2020.
- [8] N. E. Isnawati, I. Istikomah, and M. A. Khalif, "Fermion mass formulation in the Modified Left-Right Symmetry Model," *J. Nat. Sci. Math. Res.*, vol. 8, no. 2, pp. 66–74, 2022, doi: 10.21580/jnsmr.2022.8.2.13633.
- [9] A. S. Adam, A. Ferdiyan, and A. Satriawan, "A New Left-Right Symmetry Model," *Adances High Energy Phys.*, 2020.
- [10] M. Kawasaki, K. Kohri, T. Moroi, and Y. Takaesu, "Revisiting big-bang nucleosynthesis constraints on long-lived decaying particles," *Phys. Rev. D*, vol. 97, no. 2, p. 23502, 2018, doi: 10.1103/PhysRevD.97.023502.
- [11] A. Boyarsky, M. Ovchinnikov, O. Ruchayskiy, and V. Syvolap, "Improved big bang nucleosynthesis constraints on heavy neutral leptons," *Phys. Rev. D*, vol. 104, no. 2, p. 23517, 2021, doi: 10.1103/PhysRevD.104.023517.
- [12] D. Griffiths, *Introduction to Elementary Particles*, Second, Re. WILEY-VCH Verlag GmbH & Co. KGaA, 2008.
- [13] M. Satriawan, "A Multicomponent Dark Matter in a Model with Mirror Symmetry with Additional Charged Scalars," no. 1, pp. 1–9, 2018.